Perturbation Analysis of Rectangular Waveguide Containing Transversely Magnetized Semiconductor

G. J. GABRIEL AND M. E. BRODWIN, MEMBER, IEEE

Abstract—The boundary value problem of rectangular waveguide, filled with transversely magnetized semiconductor or plasma, is solved by a perturbation method reported earlier [1]. The solution by first-order theory is compared to the results of an experiment in which surface currents in the guide wall due to perturbed and unperturbed $TE_{1,0}$ wave in *N*-type Silicon are sampled and segregated. Theoretical and experimental results are in excellent agreement.

Introduction

RECENTLY we reported a general perturbation method for the analysis of waveguides containing anisotropic, inhomogeneous, dissipative media [1]. In the present work, we apply the method to rectangular waveguides filled with a gas plasma or semiconductor in a transverse magnetic field. For the purpose of demonstrating the accuracy of the first-order perturbation theory, the theoretical results are compared to the results of an experiment employing a semiconductor.

At microwave frequencies, as it is well known [2], plasmas and semiconductors in a magnetostatic field are characterized by a tensor permittivity and a tensor conductivity, respectively. The semiconductor is regarded as the solid-state counterpart of the gas plasma, since the conductivity can be considered as part of a complex permittivity tensor. Thus, the analyses of problems involving the two media are identical. We have confined the analytical development to semiconductors, since in the experimental verification it was more convenient to use a semiconductor than a gas plasma. The theoretical results and conclusions are applicable to both media.

Although the problem under consideration is presented principally as an example of a method of approximation [1], this problem has considerable practical interest. Application of a transverse magnetostatic field leads to electrically controllable phase shift and attenuation. Measured values of the propagation constant can also be used to determine the transport parameters, m^*, μ, and τ, of an unknown semiconductor. Thus, the approximate solution can be used for studying the feasibility of components and as an aid in investigating new diagnostic methods. From the latter viewpoint, the perturbation analysis is particularly advantageous, since it yields much simpler results than the exact solution, which requires all six E- and H-field components of the wave and their dependence on both coordinates in the transverse plane [3]. This is unlike the ferrite where many of the effects can be adequately explained by consideration of the restricted $TE_{0,n}$ solutions [4], [5].

The dominant $TE_{1,0}$ mode of the empty guide is usually of greatest interest in practice. The general solution does not provide simply and explicitly the connection between the characteristic waves of the anisotropic plasma or semiconductor and the $TE_{1,0}$ mode of the empty guide. It is with the perturbation method that this connection is established quantitatively. Even for the higher order modes, the expressions of the general solution are too complicated for numerical calculation in a practical situation.

We shall first briefly review the salient steps of our previous development [1]. The perturbation expressions are then derived for rectangular waveguide completely filled with a semiconductor. In the experiment, the surface currents in the guide walls under $TE_{1,0}$ excitation provide the quantitative observable which permits separation of the perturbed and unperturbed parts of the fields. Thus, the analysis ends with an expression for these currents. This is then followed by a description of the experimental scheme which, in addition to providing verification for the theory, is also another method for determining the Hall mobility of semiconductors.

Perturbation Theory

Only first-order nondegenerate perturbation is considered, the extension to higher order ones being similar in method. We shall assume all field quantities to have the dependence $\exp i(\kappa z-\omega t)$. Consider the rectangular waveguide completely filled with a semiconductor in a transverse static magnetic field, as in Fig. 1. In the absence of the magnetic field, the characteristic waves are the usual TE and TM modes. Our objective is to establish an analytic connection between the characteristic waves in the presence and absence of the perturbing magnetic field. This connection will appear as additive terms on the unperturbed TE and TM modes.

In the formalism of previous work [1], [6], the αth

Manuscript received April 23, 1965; revised October 1, 1965 and February 7, 1966. This work was supported by the Advanced Research Projects Agency, Department of Defense, through the Materials Research Center, Northwestern University.

G. J. Gabriel is with the Dept. of Electrical Engineering, University of Notre Dame, Notre Dame, Ind. He was formerly with the Dept. of Electrical Engineering, Northwestern University.

M. E. Brodwin is with the Dept. of Electrical Engineering, Northwestern University, Evanston, Ill.

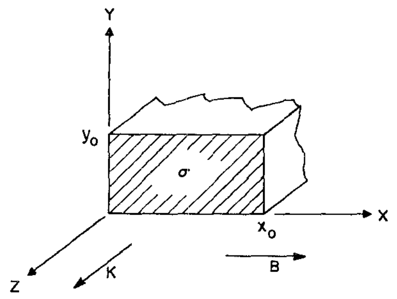

Fig. 1. Rectangular waveguide with transverse static magnetic field B.

characteristic wave is specified by the six-vector wave function

$$\Phi_\alpha = \begin{bmatrix} E_\alpha \\ iH_\alpha \end{bmatrix} \tag{1}$$

where E_α and H_α are the microwave electric and magnetic vectors. In this six-vector formalism, the Maxwell Equations appear as

$$(\mathcal{L} - \kappa_\alpha \mathbf{\Gamma})\Phi_\alpha = 0 \tag{2}$$

where

$$\mathcal{L} = \mathcal{L}_0 + L$$

$$\mathcal{L}_0 = \begin{bmatrix} \omega\epsilon_0 I & -\nabla_t \times I \\ -\nabla_t \times I & \omega\mu_0 I \end{bmatrix}$$

$$\mathbf{\Gamma} = \begin{bmatrix} 0 & i\hat{z} \times I \\ i\hat{z} \times I & 0 \end{bmatrix}. \tag{3}$$

The symbols ∇_t, I, and $\hat{z}$ are, respectively, the transverse del operator, the identity dyadic, and the unit vector along the z-axis. The operator L is the perturbation operator which embodies the anisotropy and in general is

$$L = \begin{bmatrix} \omega\epsilon_0 \chi_e & 0 \\ 0 & \omega\mu_0 \chi_m \end{bmatrix} \tag{4}$$

where χ_e and χ_m are the electric and magnetic susceptibility dyadics (tensors). In the case of the semiconductor, χ_m is zero as the permeability is assumed to be that of vacuum. The permittivity ϵ_0 is complex and it accounts for displacement as well as conduction currents.

Since the anisotropy is induced by the magnetic field, we use the field intensity as the perturbation parameter [1] and designate it by the dimensionless variable ν_c. Thus, we expand

$$L = \sum_{n=1} \nu_c^n L^{(n)} \tag{5}$$

$$\Phi_\alpha = \left[\Phi_\alpha^{(0)} + \sum_{n=1} \nu_c^n \Phi_\alpha^{(n)} \right] e^{i\kappa\alpha z} \tag{6}$$

$$\kappa_\alpha = \kappa_{\alpha 0} + \sum_{n=1} \nu_c^n \kappa_{\alpha n} \tag{7}$$

where $\kappa_{\alpha 0}$ and $\Phi_\alpha^{(0)}$ are, respectively, the zero-order eigenvalues (wave numbers) and eigenvectors (modes) of $\mathcal{L}_0$ in the absence of the magnetic field, and $\kappa_{\alpha n}$ and $\Phi_\alpha^{(n)}$ are the nth order perturbations. Our task is to determine $\Phi_\alpha^{(n)}$ and $\kappa_{\alpha n}$ which satisfy the recurrence equations,

$$\begin{aligned}
(\mathcal{L}_0 - \kappa_{\alpha 0}\mathbf{\Gamma})\Phi_\alpha^{(0)} &= 0 \\
(\mathcal{L}_0 - \kappa_{\alpha 0}\mathbf{\Gamma})\Phi_\alpha^{(1)} &= -(L^{(1)} - \kappa_{\alpha 1}\mathbf{\Gamma})\Phi_\alpha^{(0)} \\
(\mathcal{L}_0 - \kappa_{\alpha 0}\mathbf{\Gamma})\Phi_\alpha^{(2)} &= -(L^{(1)} - \kappa_{\alpha 1}\mathbf{\Gamma})\Phi_\alpha^{(1)} \\
&\quad - (L^{(2)} - \kappa_{\alpha 2}\mathbf{\Gamma})\Phi_\alpha^{(0)}.
\end{aligned} \tag{8}$$

We observe that by virtue of the linear independence of ν_c, all the $\Phi_\alpha^{(n)}$ satisfy the same boundary conditions as $\Phi_\alpha^{(0)}$ and hence they belong in the domain of $\mathcal{L}_0$. Consequently, every $\Phi_\alpha^{(n)}$ may be represented in a series of the spectral functions of $\mathcal{L}_0$.

The first-order field is then given by

$$\Phi_\alpha^{(1)} = \sum_\beta (a_{\beta 1}\Phi_\beta^{(0)} - a_{-\beta 1}\Phi_{-\beta 1}^{(0)}) \tag{9}$$

where $\Phi_{-\beta}^{(0)} = \Phi_\beta^{(0)}(-\kappa_{\beta 0})$. Both sets of functions for $\pm\beta$ must be included, since $\pm\kappa_{\beta 0}$ are both eigenvalues of $\mathcal{L}_0$. The coefficients $a_{\pm\beta 1}$ and the first- and second-order perturbations of the eigenvalues are determined by the methods outlined in [1]. Using the notation

$$L_{\beta,\alpha}^{(1)} = \langle \Phi_\beta^{(0)} \mid L^{(1)}\Phi_\alpha^{(0)} \rangle,$$

where the symmetric scalar product is defined by the integral over the cross section of the guide,

$$\langle \Phi_\beta \mid \Phi_\alpha \rangle = \int (E_\beta \cdot E_\alpha + iH_\beta \cdot iH_\alpha) da,$$

we have

$$\alpha_{\pm\beta 1} = \frac{L_{\mp\beta,\alpha}^{(1)}}{\kappa_{\alpha 0} \mp \kappa_{\beta 0}} \tag{10}$$

$$\kappa_{\alpha 1} = L_{-\alpha,\alpha}^{(1)} \tag{11}$$

$$\kappa_{\alpha 2} = L_{-\alpha,\alpha}^{(2)} + \sum_\beta{}' \frac{L_{-\beta,\alpha}^{(1)} L_{-\alpha,\beta}^{(1)}}{\kappa_{\alpha 0} - \kappa_{\beta 0}} - \sum_\beta \frac{L_{\beta,\alpha}^{(1)} L_{-\alpha,-\beta}^{(1)}}{\kappa_{\alpha 0} + \kappa_{\beta 0}}. \tag{12}$$

The prime on the summation denotes exclusion of the term $\beta = \alpha$. For a given zero-order wave, these quantities can be calculated once the dyadic coefficients $L^{(n)}$ have been determined. We shall identify $L^{(n)}$ for the semiconductor by considering the conductivity tensor.[1]

[1] For convenience we use dyadic and matrix representations interchangeably.

The Conductivity Tensor

With the magnetic field oriented along the x-axis, the semiconductor is described by the tensor[1]

$$\boldsymbol{\sigma} = \begin{bmatrix} \sigma_0 & 0 & 0 \\ 0 & \sigma_{11} & -\sigma_{12} \\ 0 & \sigma_{12} & \sigma_{22} \end{bmatrix} \tag{13}$$

where σ_0 is the high-frequency conductivity in the absence of the magnetic field. We assume the field to be parallel to the $\langle 111\rangle$ or $\langle 100\rangle$ crystallographic axes so that σ_{12} and σ_{22} are equal. It is further assumed that the diagonal element σ_{11} is an even function of the static magnetic field and the off-diagonal element σ_{12} is an odd function.

To fit the formalism of the theory, the conductivity needs to be viewed as part of a complex dyadic permittivity. Hence, we define

$$\boldsymbol{\varepsilon} = \epsilon_0 \boldsymbol{I} + \frac{i}{\omega}(\boldsymbol{\sigma} - \sigma_0 \boldsymbol{I}) \tag{14}$$

where $\epsilon_0 = \epsilon_s + (i/\omega)\sigma_0$ is the high-frequency scalar permittivity in the absence of the magnetic field, and ϵ_s is the static permittivity of the host crystal which does not include any polarization contribution from the carriers.

The dyadic (tensor) permittivity is now in the desired form. The first term in (14) is the isotropic part and the second term accounts for the anisotropy induced by the magnetic field. Thus, we identify $\boldsymbol{L}$ by comparison to (4),

$$\boldsymbol{L} = i\begin{bmatrix} \boldsymbol{\sigma} - \sigma_0 \boldsymbol{I} & 0 \\ 0 & 0 \end{bmatrix}. \tag{15}$$

To obtain the dyadic coefficients $\boldsymbol{L}^{(n)}$, we expand $\boldsymbol{\sigma} - \sigma_0 \boldsymbol{I}$ about $\nu_c = 0$, it being understood that $\boldsymbol{\sigma}$ is a known function of the magnetic field. Since σ_{11} and σ_{12} are even and odd functions of ν_c, we have

$$\boldsymbol{\sigma} - \sigma_0 \boldsymbol{I} = \sum_{n=1} \overset{(2n)}{\sigma_{11}} \nu_c^{2n} \boldsymbol{I}_s + \overset{(2n-1)}{\sigma_{12}} \nu_c^{2n-1} \boldsymbol{I}_a \tag{16}$$

where $\boldsymbol{I}_s$ and $\boldsymbol{I}_a$ are the special 3 by 3 matrices

$$\boldsymbol{I}_s = \begin{bmatrix} 0 & 0 & 0 \\ 0 & 1 & 0 \\ 0 & 0 & 1 \end{bmatrix} \qquad \boldsymbol{I}_a = \begin{bmatrix} 0 & 0 & 0 \\ 0 & 0 & -1 \\ 0 & 1 & 0 \end{bmatrix}.$$

Comparison of (15) and (16) with (5) shows that

$$\boldsymbol{L}^{(1)} = i\overset{(1)}{\sigma_{12}} \begin{bmatrix} \boldsymbol{I}_a & 0 \\ 0 & 0 \end{bmatrix} \tag{17}$$

$$\boldsymbol{L}^{(2)} = i\overset{(2)}{\sigma_{11}} \begin{bmatrix} \boldsymbol{I}_s & 0 \\ 0 & 0 \end{bmatrix} \tag{18}$$

with similar expressions for the higher order coefficients. Thus, for the semiconductor,

$$L^{(1)}_{\pm\beta,\alpha} = i\overset{(1)}{\sigma_{12}} \int E^{(0)}_{\pm\beta} \cdot \boldsymbol{I}_a \cdot E^{(0)}_{\alpha} \, da. \tag{19}$$

Expression (19), together with (10), shows that the first-order perturbation of the fields is dependent on the off-diagonal element of the conductivity tensor. It is also worth noting that thus far it has not been necessary to adopt a particular relationship between the conductivity elements and the transport parameters. The form of the elements depends on the particular model adopted for the description of carrier diffusion within the crystal or plasma. We shall use the Drude-Zener model when we correlate the experimental and theoretical results.

Excitation with $TE_{p,0}$ Modes

We consider now the case of propagation of the $TE_{p,0}$ mode whose electric vector is parallel to the y-axis. It must be emphasized that the preceding development is not applicable to the $TE_{p,q}$ modes, since these are degenerate with the $TM_{p,q}$ modes and require treatment by degenerate perturbation theory [7]. Only one mode $(p, 0)$ is assumed to be propagating, and we wish to determine the first-order perturbation of this wave. For convenience of notation, we use the indexes $\alpha = (p, 0)$ and $\beta = (m, n)$.

For the TE_α modes, the axial component $E^{(0)}_{\alpha z}$ is identically zero; and since $E^{(0)}_{-\beta z} = -E^{(0)}_{\beta z}$, then $L^{(0)}_{\beta,\alpha}$ in (19) reduces to

$$L^{(1)}_{\pm\beta,\alpha} = \pm\, i\overset{(1)}{\sigma_{12}} \int E^{(0)}_{\beta z} E^{(0)}_{\alpha y} \, da. \tag{20}$$

It is evident that only the TM_β functions are significant in the first-order perturbation of $TE_{p,0}$ mode. Moreover, for the $TE_{0,q}$ modes, whose electric vectors are parallel to the x-axis and the static field, $L^{(0)}_{\beta,\alpha}$ vanishes and there is no perturbation.

The TM_β spectral functions are derived from the normalized scalar functions [8],

$$\psi_\beta = \left[-\tfrac{1}{2}\omega\epsilon_0\kappa_{\beta 0}k_\beta^2 x_0 y_0\right]^{-1/2} \sin\frac{m\pi}{x_0}x \sin\frac{n\pi}{y_0}y, \tag{21}$$

where the normalization condition is

$$\langle \Phi^{(0)}_{-\beta} \mid \Gamma \Phi^{(0)}_{\beta} \rangle = 1$$

and

$$k_\beta^2 = \left(\frac{m\pi}{x_0}\right)^2 + \left(\frac{n\pi}{y_0}\right)^2.$$

In terms of these functions, the first-order field may be expressed now in component form by substitution of (20) and (10) into (9) and utilization of the "reflection symmetry" property of the spectral functions. The desired result is

$$\Phi_\alpha^{(1)} = -i\sigma_{12}^{(1)} 2 \sum_\beta \frac{\int E_{\beta z}^{(0)} E_{\alpha y}^{(0)} da}{\kappa_{\alpha 0}^2 - \kappa_{\beta 0}^2} \kappa_{\beta 0} \begin{bmatrix} i\kappa_{\alpha 0} \frac{\partial \psi_\beta}{\partial x} \\ i\kappa_{\alpha 0} \frac{\partial \psi_\beta}{\partial y} \\ k_\beta^2 \psi_\beta \\ \omega\epsilon_0 \frac{\partial \psi_\beta}{\partial y} \\ -\omega\epsilon_0 \frac{\partial \psi_\beta}{\partial x} \\ 0 \end{bmatrix}. \quad (22)$$

In this sum only the terms $\beta = (1, 2m+1)$ are nonvanishing. The complete αth quasi-mode, to first-order approximation, is then given by

$$\Phi_\alpha{}^{(1)} = [\Phi_\alpha{}^{(0)} + \nu_c \Phi_\alpha{}^{(1)}] e^{i\kappa_{\alpha 0} z}. \quad (23)$$

Here, we have used the fact that $\kappa_{\alpha 1}$, the first-order perturbation of the wave number, vanishes for all the $TE_{p,0}$ modes. This may be readily shown from (19). The second-order perturbation may be calculated from (12). For the $TE_{1,0}$ mode, it is

$$\kappa_{\alpha 2} = \frac{i\omega\mu_0}{2\kappa_{\alpha 0}} \sigma_{11}^{(2)} + \frac{\mu_0}{2\epsilon_0 \kappa_{\alpha 0}} \left[1 + \frac{\pi^2}{12} \left(\frac{y_0}{x_0} \right)^2 \right] [\sigma_{12}^{(1)}]^2. \quad (24)$$

Wall Current for $TE_{1,0}$ Mode

In the experiment to be described in the following section, the surface currents in the guide walls were utilized as the quantitative measure of the perturbed fields. The axial component of the current density is equal to the x component of the magnetic intensity at the wall. Thus, from (22), the magnetic intensity component is, for $\alpha = (1, 0)$,

$$\nu_c H_{\alpha x}^{(1)} = -2\nu_c \sigma_{12}^{(1)} \omega\epsilon_0 \sum_\beta \frac{\int E_{\beta z}^{(0)} E_{\alpha y}^{(0)} da}{\kappa_{\alpha 0}^2 - \kappa_{\beta 0}^2} \kappa_{\beta 0} \frac{\partial \psi_\beta}{\partial y} \cdot \quad (25)$$

The exact evaluation of this integral and sum (Appendix, Section A) leads to

$$\nu_c H_{\alpha x}^{(1)} = -a_{1,0} i\omega\mu_0 \nu_c \sigma_{12}^{(1)} \frac{\pi}{x_0} (y - \tfrac{1}{2} y_0) \sin \frac{\pi}{x_0} x \quad (26)$$

where $a_{1,0}$ is the arbitrary amplitude of the initial $TE_{1,0}$ wave. Thus, in the broad walls $y = (0, y_0)$, the first-order perturbation of the axial current density is

$$\nu_c J_{\alpha z}^{(1)} = \frac{1}{2} a_{1,0} i\omega\mu_0 \nu_c \sigma_{12}^{(1)} y_0 \frac{\pi}{x_0} \sin \frac{\pi}{x_0} x. \quad (27)$$

For measurement purposes, the ratio of this current to the unperturbed current $J_{\alpha z}^{(0)}$ is more desirable, since it is independent of the amplitude. This ratio is given by

$$\frac{\nu_c J_{\alpha z}^{(1)}}{J_{\alpha z}^{(0)}} = \frac{\omega\mu_0}{2\kappa_{1,0}} y_0 \sigma_{12}^{(1)} \nu_c. \quad (28)$$

It is this ratio that is observed in the experiment. Numerical values for N-type Silicon at room temperature are computed in the Appendix, Section B.

Experimental Method and Results

The purpose of the experiment is to determine the range of validity of the first-order perturbation theory of the preceding sections. The theory of measurement is considered first, followed by presentation and discussion of the results.

The measurement of the wall current ratio is accomplished by observing the amplitudes of the fields coupled into auxiliary waveguides through slits. A narrow slit, Fig. 2, is cut in both of the broad walls of the waveguide containing the semiconductor such that they lie in the same transverse plane and are perpendicular to the axis of the guide. Each slit couples the waveguide to a secondary one, the entire configuration forming a four-port E-plane junction.

Let $J^{(0)}$ and $J^{(1)}$ be the surface currents due to the $TE_{1,0}$ mode and $TM_{1,2m+1}$ spectral functions, respectively. Since the $TE_{1,0}$ currents in the two slits are out of phase by 180 degrees and the $TM_{1,2m+1}$ currents are in phase, the wave amplitudes coupled into one arm of the junction, say arm A, is

$$Q_A = C(J^{(1)} + J^{(0)}) \quad (29)$$

and in arm B is

$$Q_B = C(J^{(1)} - J^{(0)}) \quad (30)$$

where C is a coupling coefficient. By forming the phasor sum and difference of these two signals, the current amplitudes are separated. A microwave bridge is employed to perform this operation. The two side arms of the slit coupled junction feed into arms 1 and 2 of the matched hybrid junction via adjustable attenuators and phase shifters as shown in Fig. 3.

In the absence of the static magnetic field, only the $TE_{1,0}$ mode is present in the semiconductor, so that

$$Q_A = -Q_B = CJ^{(0)}.$$

The phase shifter and attenuators are adjusted for a null in the H-port of the first bridge. The output in the E-port of that bridge is then $2CJ^{(0)}$. Some adjustment of the attenuators is necessary because perfect symmetry of the four-arm junction is not possible practically.

When the magnetic field is applied, the current due to the $TM_{1,2m+1}$ spectral functions appears and the signals are then as in (29) and (30). Since the bridge is adjusted for the sum of Q_A and Q_B in the H-port, the output in this arm is

$$Q_A + Q_B = 2CJ^{(1)},$$

and in the E-port it is

$$Q_A - Q_B = 2CJ^{(0)}.$$

Measurement of the absolute values of the coupled power is cumbersome, since it requires a determination of the slit coupling coefficient. Moreover, because of magnetoresistance, the effects are obscured since the amplitudes $J^{(0)}$ with and without the magnetic field are different. The ratio of $J^{(1)}$ to $J^{(0)}$, however, is independent of both the coupling coefficient and the amplitude of $J^{(0)}$.

The ratio is measured by means of a second bridge. The signals Q_A+Q_B and Q_A-Q_B are fed into arms 1' and 2', respectively, of a second matched hybrid junction. In the branch carrying Q_A-Q_B, an adjustable precision attenuator is interposed, while in the branch with Q_A+Q_B, a phase shifter is inserted. The E' arm of the second junction leads to the null detector, and the H' arm is terminated in a matched load.

Let R be the multiplicative factor by which the precision attenuator reduces the signal amplitude. Then the detector, being in the E' arm, picks up the signal

$$Q_D = 2RCJ^{(0)} - 2CJ^{(1)}.$$

When the phase shifter and the precision attenuator are so adjusted that the signals arriving at the junction are of equal amplitude and phase, Q_D vanishes. Hence, we have the condition

$$R = \left| \frac{J^{(1)}}{J^{(0)}} \right|.$$

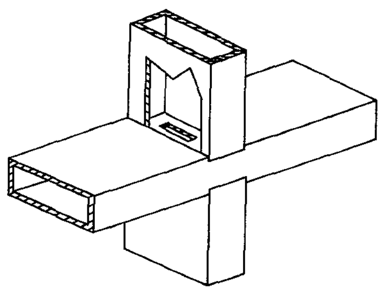

Fig. 2. The slit-coupled four-port E-plane junction.

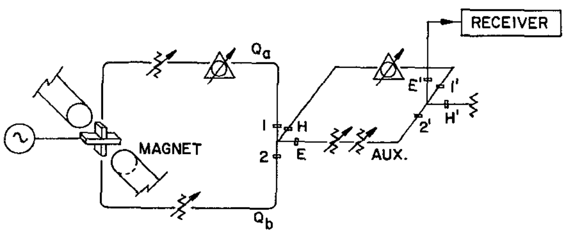

Fig. 3. A schematic diagram of the double bridge method of measurement.

Thus, the attenuator readings give the desired current ratio.

Experimental Results

The current ratio was observedi n 11.1 ohm-cm and 3.1 ohm-cm N-type Silicon which completely filled a section of standard K-band waveguide. The operating frequency was 22.235 Gc/s and the temperature 32°C. The measured wall current ratio as a function of the applied magnetic field is shown in Fig. 4 for a range zero to 10 kilogauss. The spread in the data for the 3.1 ohm-cm is due to reduced power level resulting from extreme attenuation. It is seen that the data fit remarkably well on straight lines whose slopes are computed from the Drude-Zener model in the Appendix, Section B. The linearity of the data and the close fit to the theoretical slopes of the lines demonstrate the excellent accuracy of the first-order perturbation method in the low magnetic field region.

Because of severe discontinuity at the semiconductor-air interface, the perturbation theory of the infinitely long waveguide leads to a discrepancy in regions near the interface. This discrepancy disappears at distances, defined in Fig. 4, which are greater than two guide wavelengths in the semiconductor. The observed current ratio increases with s and asymptotically approaches the theoretical values.

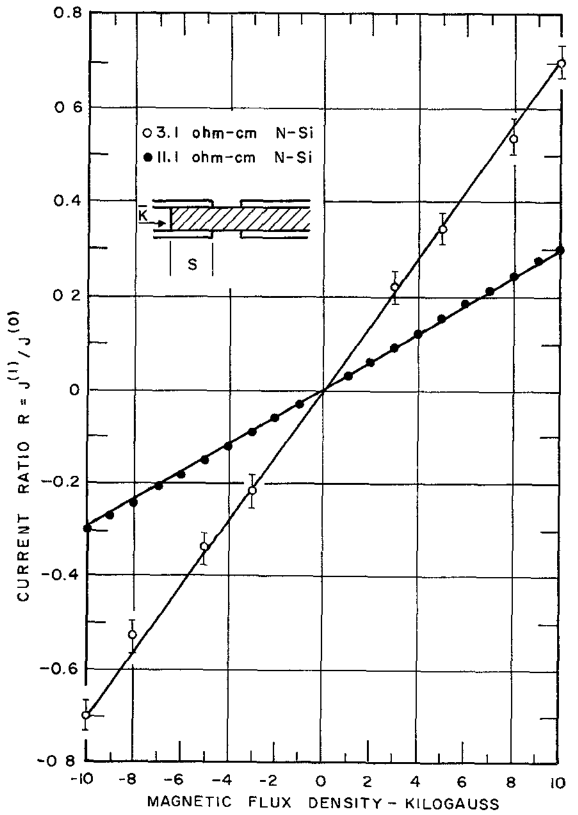

Fig. 4. TE-TM current ratio as function of the magnetic field in N-type Silicon at 32°C, s = 7.0 mm, B along ⟨111⟩ axis.

Conclusion

The perturbation method and equivalent variational forms [1] appear to be the only comparatively simple and accurate methods for analysis of transversely magnetized plasma and semiconductor in rectangular waveguide. The first-order perturbation approximation was shown to be in excellent agreement with experimental results. The experimental scheme also provides another method for measurement of the Hall mobility at room temperature and low magnetic intensity.

It must be emphasized that the perturbation equations are valid for all cylindrical waveguides containing plasma or semiconductor, without regard to direction of magnetization, provided the material properties are independent of the axial coordinate. The method can be used as long as the series (5) for the operator L is available. Accuracy of the results and rapidity of convergence of the perturbation terms can be assured by simply maintaining the physical parameter ν_c within prescribed bounds.

Appendix

A. Evaluation of the Sum (25)

The TM_β spectral functions are defined by

$$\Phi_\beta{}^{(0)} = \begin{bmatrix} \dfrac{\nabla \times \nabla \times \hat{z}\psi_B}{\omega\epsilon_0 \nabla \times \hat{z}\psi_\beta} \end{bmatrix}$$

where

$$\psi_\beta = a_\beta \sin \frac{m\pi}{x_0} x \sin \frac{n\pi}{y_0} y$$

$$a_\beta = \left[-\tfrac{1}{2}\omega\epsilon_0\kappa_{\beta 0}k_\beta{}^2 x_0 y_0\right]^{-1/2}$$

$$\kappa_{\beta 0}{}^2 = \omega^2\mu_0\epsilon_0 - k_\beta{}^2.$$

The $TE_{1,0}$ field, $\alpha=(1, 0)$, is defined by

$$H_{\alpha z}^{(0)} = a_{1,0}k_{1,0}^2 \cos \frac{\pi}{x_0} x$$

$$H_{\alpha x}^{(0)} = -i\kappa_{1,0}a_{1,0}\frac{\pi}{x_0} \sin \frac{\pi}{x_0} x$$

$$E_{\alpha y}^{(0)} = i\omega\mu_0 a_{1,0}\frac{\pi}{x_0} \sin \frac{\pi}{x_0} x.$$

Thus

$$\int E_{\beta z}^{(0)} E_{\alpha y}^{(0)} da$$

$$= i\omega\mu_0 a_{1,0} a_\beta k_\beta{}^2 \frac{\pi}{x_0}$$

$$\times \int_0^{x_0}\int_0^{y_0} \sin\frac{\pi x}{x_0} \sin\frac{m\pi x}{x_0} \sin\frac{n\pi y}{y_0} dx dy$$

$$= i\omega\mu_0 a_{1,0} a_\beta k_\beta{}^2 \frac{y_0}{2n}\left[1 - (-1)^n\right]; \qquad \beta = (1, n).$$

Substitution of this integral in (25) gives

$$H_{\alpha x}^{(1)}\nu_c = 4i\omega\mu_0 a_{1,0}\sigma_{12}^{(1)}\nu_c \frac{\pi}{x_0} \sin\frac{\pi x}{x_0} \sum_{n=1,3,\cdots} \frac{y_0}{n^2\pi^2}\cos\frac{n\pi}{y_0} y.$$

It can be shown that the last sum is

$$\tfrac{1}{4}(y - \tfrac{1}{2}y_0) = -\frac{y_0}{\pi^2}\sum_{n=1,3,\cdots}\frac{1}{n^2}\cos\frac{n\pi}{y_0} y.$$

The ratio of $H_{\alpha x}{}^{(0)}\nu_c$ to $H_{\alpha x}{}^{(0)}$ gives (28).

B. Numerical Values for the Current Ratio

Using the semiclassical Drude-Zener Model [9], one can show that

$$\sigma_{11} = \sigma_{dc}\frac{1 - i\omega\tau}{(1 - i\omega\tau)^2 + \mu_H{}^2B^2}$$

$$\sigma_{12} = \sigma_{dc}\frac{\mu_H B}{(1 - i\omega\tau)^2 + \mu_H{}^2B^2}$$

where μ_H is the Hall Mobility, B is the static magnetic induction, τ is the energy-independent collision time, and $\sigma_{dc} = e^2\tau\, n/m^*$ is the dc conductivity. In the absence of magnetic field, σ_{12} vanishes and σ_{11} reduces to the high-frequency conductivity,

$$\sigma_0 = \frac{\sigma_{dc}}{1 - i\omega\tau}.$$

Consider the element σ_{12} which may be put in the form

$$\sigma_{12} = \frac{\sigma_0}{1 - i\omega\tau}\,\frac{\mu_H B}{1 + \left[\dfrac{\mu_H B}{1 - i\omega\tau}\right]^2}.$$

This can be expanded as

$$\sigma_{12} = \frac{\sigma_0}{1 - i\omega\tau}\left[\mu_H B - \frac{(\mu_H B)^3}{(1 - i\omega\tau)^2} + \cdots\right].$$

If we take $\nu_c = \mu_H B$, we have

$$\sigma_{12}^{(1)} = \frac{\sigma_0}{1 - i\omega\tau}.$$

Thus, the current ratio in (28) becomes

$$R = \left|\frac{\nu_c J_{\alpha z}^{(1)}}{J_{\alpha z}^{(0)}}\right| = \left|\frac{\omega\mu_0\sigma_0 y_0}{2\kappa_{1,0}(1 - i\omega\tau)}\mu_H B\right|.$$

In particular, at room temperature where $\omega\tau \ll 1$, we have

$$R = \left|\frac{\omega\mu_0\sigma_{dc}y_0}{2\kappa_{1,0}}\mu_H B\right|.$$

This expression is used to calculate the ratio for N-type silicon with resistivities 11.1 ohm-cm and 3.1 ohm-cm. In computing $|\kappa|$, it is recalled that ϵ_0 was defined by

$$\epsilon_0 = \epsilon_s + i\frac{\sigma_0}{\omega}$$

where $\epsilon_s = \epsilon_r\epsilon_v$ and ϵ_v is the permittivity of vacuum. At room temperature σ_0 reduces to σ_{dc}. Thus,

$$\kappa^2 = \omega^2\mu_0\epsilon_0 - k^2$$

leads to

$$|\kappa| = \frac{2\pi}{\lambda_0}\left\{[1 - (\lambda_0/\lambda_c)^2]^2 + [\sigma_{dc}/\omega\epsilon_s]^2\right\}^{1/4}$$

where $2\pi/\lambda_0 = \omega\sqrt{\mu_0\epsilon_s}$ and $\lambda_c = 2\pi/k$.

The following numerical values were used in the calculation:

$$\epsilon_r = 12 \qquad f = 22.235 \text{ Gc/s}$$
$$\mu_H = 1450 \text{ cm}^2/\text{volt-s} \qquad \lambda_0 = 0.388 \text{ cm}$$
$$B = 10 \text{ kilogauss} \qquad \lambda_c = 2.14 \text{ cm}$$
$$y_0 = 0.43 \text{ cm}.$$

The resulting values for the ratio are

$$R = 0.288 \qquad \text{for 11.1 ohm-cm}$$
$$R = 0.709 \qquad \text{for 3.1 ohm-cm.}$$

Calculations on the basis of a model using the Boltzmann transport equation [10] lead to results which are smaller than the above values by a factor of 0.88 or 1.1 dB.

References

[1] G. J. Gabriel and M. E. Brodwin, "The solution of guided waves in inhomogeneous anisotropic media by perturbation and variational methods," *IEEE Trans. on Microwave Theory and Techniques*, vol. MTT-13, pp. 364–370, May 1965.
[2] B. Lax and L. M. Roth, "Propagation and plasma oscillations in semiconductors with magnetic fields," *Phys. Rev.*, vol. 98, pp. 548–549, 1955.
[3] G. J. Gabriel and M. E. Brodwin, "Distinctions between gyroelectric and gyromagnetic media in rectangular waveguide," this issue, page 292.
[4] P. H. Vartanian and E. T. Jaynes, "Propagation in ferrite-filled transversely magnetized waveguide," *IRE Trans. on Microwave Theory and Techniques*, vol. MTT-4, pp. 140–143, July 1956.
[5] B. Lax and K. J. Button, *Microwave Ferrites and Ferrimagnetics*. New York: McGraw-Hill, 1962, ch. 9, p. 355.
[6] A. D. Bresler, G. H. Joshi, and N. Marcuvitz, "Orthogonality properties for modes in passive and active uniform waveguides," *J. Appl. Phys.*, vol. 29, pp. 794–799, May 1958.
[7] G. J. Gabriel, Ph.D. dissertation, Northwestern University, Evanston, Ill., August 1964.
[8] R. E. Collin, *Field Theory of Guided Waves*. New York: McGraw-Hill, 1960, ch. 5, p. 170.
[9] J. K. Furdyna and S. Broesma, "Microwave Faraday effect in silicon and germanium," *Phys. Rev.*, vol. 120, pp. 1995–2003, December 1960.
[10] T. Burgess, Ph.D. dissertation, Northwestern University, Evanston, Ill., June 1965.

Log-Periodic Transmission Line Circuits—Part I: One-Port Circuits

R. H. DuHAMEL, FELLOW, IEEE, AND M. E. ARMSTRONG, MEMBER, IEEE

Abstract—A theoretical study of one-port log-periodic circuits consisting of a transmission line shunt loaded with open-circuit transmission lines is reported. The objective was to determine the conditions under which the phase of the input reflection coefficient varies linearly with the logarithm of the frequency. Precise definitions and general analytical techniques for log-periodic circuits are given. Results of extensive numerical calculations are presented to illustrate the dependence of the input reflection coefficient on the various design parameters. It was found that phase deviations from linear on the order of one degree are quite easily achieved.

Manuscript received October 21, 1965; revised February 17, 1966.
The authors are with the Hughes Aircraft Company, Ground Systems Group, Fullerton, Calif.

I. Introduction

THE OBJECTIVES here are to introduce and explain new concepts for transmission line circuits which are constructed according to log-periodic design principles. As with the corresponding log-periodic antennas, these circuits provide essentially frequency-independent performance over any desired finite bandwidth. Figure 1 illustrates strip line versions of the four types of circuits to be discussed. The lines in the drawings represent strips which may be inserted between parallel ground planes. The one-port circuit of Fig. 1(a), which is the subject of this report, can be de-